Thermodynamics of Cationic Lipid-DNA Complex Formation as Studied by Isothermal Titration Calorimetry

Edwin Pozharski and Robert C. MacDonald
Department of Biochemistry, Molecular Biology and Cell Biology, Northwestern University, Evanston, Illinois 60208 USA

ABSTRACT The detailed analysis of the cationic lipid-DNA complex formation by means of isothermal titration calorimetry is presented. Most experiments were done using 1,2-dioleyl-*sn*-glycero-3-ethylphosphocholine (EDOPC), but basic titrations were also done using DOTAP, DOTAP:DOPC, and DOTAP:DOPE mixtures. Complex formation was endothermic with less than 1 kcal absorbed per mole of lipid or DNA charge. This enthalpy change was attributed to DNA-DNA mutual repulsion within the lamellar complex. The exception was DOTAP:DOPE-containing lipoplex for which the enthalpy of formation was exothermic, presumably because of DOPE amine group protonation. Experimental conditions, namely, direction and titration increment as well as concentration of titrant, which dictate the structure of resulting lipoplex (whether lamellar complex or DNA-coated vesicle), were found to affect the apparent thermodynamics of complex formation. The structure, in turn, influences the biological properties of the lipoplex. If the titration of lipid into DNA was carried out in large increments, the ΔH was larger than when the injection increments were smaller, a finding that is consistent with increased vesicle disruption under large increments and which is expected theoretically. Cationic lipid-DNA binding was weak in high ionic strength solutions, however, the effective binding constant is within micromolar range because of macromolecular nature of the interaction.

INTRODUCTION

Cationic lipids as nonviral genetic material carriers (Felgner et al., 1987) are widely used in a variety of transfection and gene therapy applications. Despite significant advances in both biomedical applications and biophysical studies of these cationic lipid-DNA complexes, there remain questions about the physical mechanisms of the complex formation and the relationship between delivery efficiency and the microscopic and macroscopic structure of the complex. Which structural parameters are the most important for efficient delivery of the genetic material into living cells (Koltover et al., 1998; Kreiss et al., 1999; Ross and Hui, 1999; Xu et al., 1999; Yang and Huang, 1997; Zuidam et al., 1999)? Do other compounds exhibit structural behavior like that of the few well-studied cases (largely DOTAP (Koltover et al., 1999))? What are the specific pathways of the complex formation (Huebner et al., 1999; Kennedy et al., 2000; Oberle et al., 2000)? What is the driving force of the complex formation—counterion release (Wagner et al., 2000) or dehydration of the macromolecules (Hirsch-Lerner and Barenholz, 1999)?

Cationic lipid-DNA complex (lipoplex) formation, like any association process, is governed by thermodynamics, requiring a decrease of free energy for the process to be spontaneous. Both theoretical (Bruinsma, 1998; Dan, 1997; Harries et al., 1998; May and Ben-Shaul, 1997; May et al., 2000) and experimental (Barreleiro et al., 2000; Kennedy et al., 2000; Lobo et al., 2001; Pector et al., 2000; Spink and Chaires, 1997; Zantl et al., 1999) thermodynamic analyses have appeared, however, a detailed analysis of the heat effects of the complex formation by means of isothermal titration calorimetry (ITC) has yet to be reported. In this paper we present the results of the application of ITC to the investigation of the process of cationic lipid-DNA complex formation. Two cationic lipids were investigated. One, DOTAP, is an amphipathic cation consisting of oleic acid chains esterified to a trimethylammonium moiety (Leventis and Silvius, 1990). The second, EDOPC, is a derivative of dioleyoylphosphatidylcholine in which the phosphate oxygen anion is substituted with an ethyl group, which eliminates the negative charge of the zwitterion, yielding a structure very similar to the membrane phospholipid but having a positive charge (MacDonald et al., 1999a).

MATERIALS AND METHODS

Materials

Herring sperm DNA (Life Technologies Inc., Gaithersburg, MD) was used in all ITC experiments. According to the manufacturer, the DNA was sheared to sizes ≤2 kb and accordingly may be described as short linear DNA. Its concentration was determined by absorbance at 260 nm and expressed as the concentration of nucleotides (using average molecular weight of 330).

1,2-Dioleyl-*sn*-glycero-3-ethylphosphocholine (EDOPC) was synthesized and purified as described (MacDonald et al., 1999a). 1,2-Dioleyl-3-trimethylammonium-propane (DOTAP), 1,2-dioleyl-*sn*-glycero-3-phosphocholine (DOPC), and 1,2-dioleyl-*sn*-glycero-3-phosphoethanolamine (DOPE) were purchased from Avanti Polar Lipids (Alabaster, AL) and

Submitted September 28, 2001, and accepted for publication January 16, 2002.

Edwin Pozharski's present address is Brandeis University, Rosenstiel Basic Medical Research Center, MS-029, 415 South Street, Waltham, MA 02454-9110.

Address reprint requests to Robert C. MacDonald, Northwestern University, Department of Biochemistry, 2153 N. Campus Dr., Evanston, IL 60208-3500. Tel.: 847-491-5062; Fax: 847-467-1380; E-mail: macd@northwestern.edu.

0006-3495/02/07/556/10 $2.00

used without further purification. Lipid concentrations were determined by phosphate assay (Bartlett, 1959).

Appropriate aliquots of lipid stock solutions (generally in chloroform) were placed in a vial and excess solvent removed under an argon stream. After at least 2 h under high vacuum, the lipid film was hydrated with the appropriate buffer and briefly vortexed. Then, if necessary, bath sonication or extrusion through 100-nm polycarbonate filter (Nucleopore, Cambridge, MA) was performed as described (MacDonald et al., 1991), using a single filter. These three types of preparation are referred to as vortexed, sonicated, and extruded vesicles hereafter. Lipid vesicle size was determined by dynamic light scattering.

Buffer containing 20 mM HEPES (Fluka, Milwaukee, WI), 0.1 mM EDTA (Sigma, St. Louis, MO), pH 7.5, was used with appropriate amounts of NaCl added to adjust the ionic strength of the solution. NaCl-free buffer is referred as HE, and otherwise as *X* HE-S, in which *X* denotes the millimolar concentration of NaCl.

Isothermal titration calorimetry

The enthalpy change upon the interaction between cationic lipid and DNA was determined using a MicroCal isothermal titration calorimeter MSC-ITC (Northampton, MA) (Wiseman et al., 1989). Most experiments were done at 30°C in 150 mM HE-S buffer. Raw data were converted into injection heats using Microcal Origin 5.0 software provided by MicroCal (the procedure includes the approximation of the baseline and the integration of the heat absorbance or release peaks). The dilution heat was usually estimated from the "beyond-the-endpoint" part of the calorimetric profile, a procedure verified in numerous separate dilution runs. Then the dilution heat was subtracted and the heat effect of complex formation so obtained was integrated over the titration range.

In most cases the final integral heat curve had the shape of two intersecting straight lines (for an example of raw data and integral heat curve, see Fig. 1), the first part represents the constant slope up to the calorimetric endpoint and the second part represents the absence of additional heat absorbed or released as a result of the complex formation. We obtained estimates of both initial slope (also referred to as binding enthalpy) and calorimetric endpoint by minimizing root-mean-square deviations of the experimental curve from two intersecting straight lines.

A comment about dimensions is appropriate. If, for instance, lipid is titrated into DNA, the heat per injection is calculated in calorie/mole of lipid electrostatic charges, and the differential calorimetric profile is plotted versus the lipid:DNA charge ratio (L:D). By integrating injection heats, one obtains the integral curve, wherein the total heat absorbed or released up to particular charge ratio (in this case, in calorie/mole of DNA charges) is plotted. Thus, when the initial slope of the integral profile is obtained, it is again in calorie/mole of lipid charges and represents the constant amount of heat involved in the association of 1 mol of lipid charges with the complex.

Dynamic light scattering

Dynamic light scattering measurements were done with a Brookhaven Instruments BI-200SM goniometer and BI-9000 digital correlator (Brookhaven, NY). A Lexel 95, 3-watt argon laser (Lexel Laser Inc., CA) was the source of 514-nm light. At least 10 correlation curves with collection times long enough to provide good statistics were obtained for all tested samples. Effective diameter was calculated by the cumulants method (Koppel, 1972) and then averaged, thus giving an estimate of the experimental uncertainty.

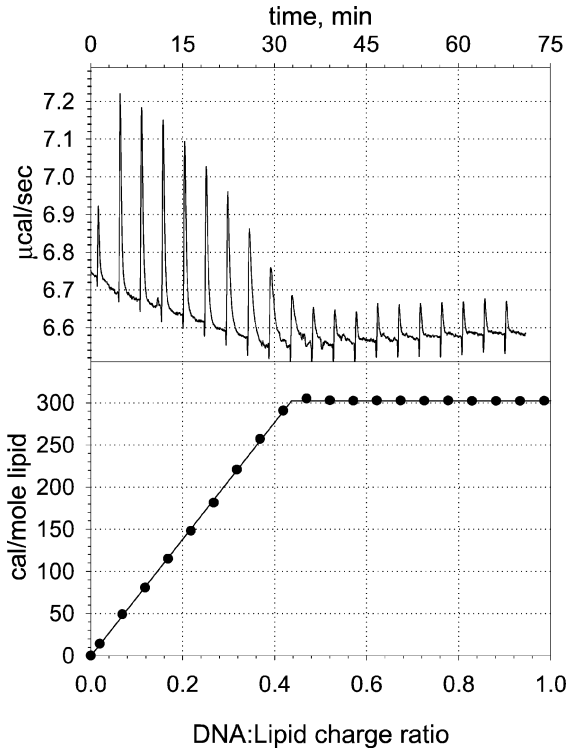

FIGURE 1 An example of the calorimetric profile. Herring DNA (2.3 mM) was titrated into 1.34 mL of 175 μM vortexed EDOPC vesicle suspension (30°C, 150 mM HE-S). (*Upper panel*) Raw data. The first injection was 2 μL, all others 5 μL, with 3.5-min interval between injections. (*Lower panel*) Integral heat versus D:L charge ratio. The solid curve represents the results of fitting by two intersecting straight lines.

RESULTS

Extruded lipid (EDOPC) injected into DNA solution: the slope of the calorimetric profile is related to the titration increment size

We carried out 19 titrations of extruded EDOPC vesicles into DNA solution, varying both DNA concentration (15.5–300 μM) and the amount of lipid per injection. The temperature was held at 30°C, and 150 mM HE-S was the buffer. All the curves were represented quite well by two intersecting straight lines, thus yielding values of the initial slope and the position of the titration endpoint. Thus, we obtained two parameters (DNA concentration and the titration increment size, expressed as the number of steps to reach a 1:1 charge ratio, i.e., the neutralization point) and two independently measured values (initial slope of the calorimetric profile and the calorimetric endpoint).

All four possible pairs of experimental parameters and measured values were tested for correlation; the highest was that between binding enthalpy and titration increment. As can be seen from Fig. 2, the experiments fall into two clusters corresponding to "small" and "large" increment titrations; 13 results with a slope lower than 595 cal/mol lipid were all obtained from experiments in which the

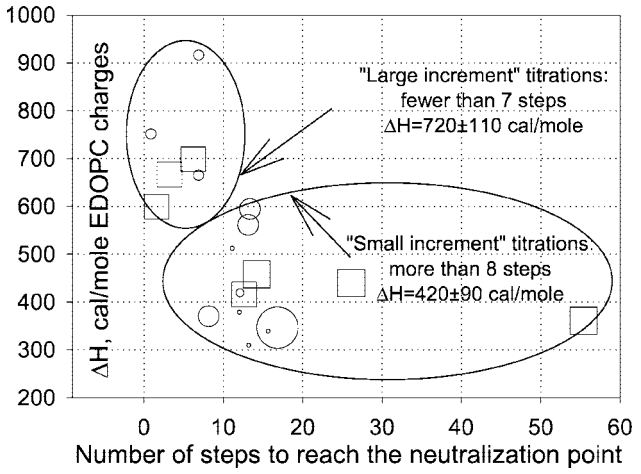

FIGURE 2 Extruded EDOPC vesicles were titrated into herring DNA at 30°C, 150 mM HE-S. The slope of the calorimetric profile is plotted versus the number of steps to reach the neutralization point. Squares correspond to the set of titrations specifically performed with the same sample at different increments to clarify the effect of the titration increment. The size of the symbols is proportional to the concentration of DNA. The boundary between the two clusters is at approximately seven steps.

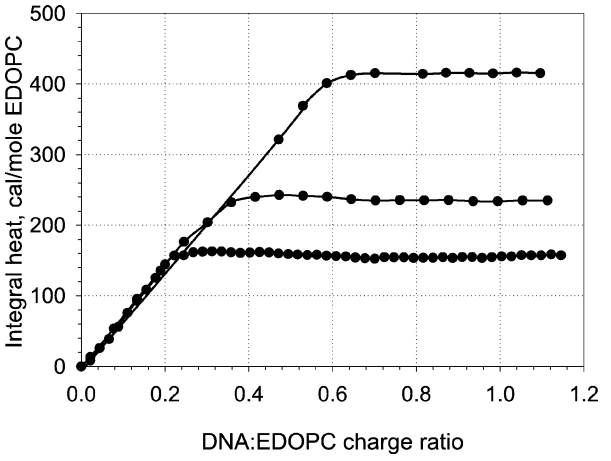

FIGURE 3 Titration of herring DNA into an extruded EDOPC vesicle suspension. In all three runs 2.3 mM DNA was injected into 155 μM lipid (T = 30°C, 150 mM HE-S). The same lipid and DNA solutions were used for all runs.

neutralization point was reached in eight or more steps, whereas six others with higher slope were all from experiments in which seven or fewer steps were involved. Average binding enthalpies were 420 ± 90 cal/mol lipid and 720 ± 110 cal/mol lipid for the "small" and "large" increment titrations, respectively. Thus, when lipid was added to DNA, the absorbed heat was 1.7 ± 0.5 times larger for the "large" increment additions than for the "small" increment additions.

The average calorimetric endpoint (as moles lipid/moles DNA) was 1.22 ± 0.19 (D:L = 0.82 ± 0.13) and 1.33 ± 0.34 (D:L = 0.75 ± 0.19) for the "small" and "large" increment titrations, respectively. No significant correlation between the endpoint and either the titration increment or the binding enthalpy was found, but some correlation with DNA concentration was noted. Two aspects of these experiments are noteworthy: 1) the endpoint was shifted to higher lipid:DNA charge ratios as the DNA concentration was increased and 2) "small" increment titration endpoints correlated with DNA concentration, whereas those of the "large" increment titrations were more or less independent of it.

DNA injected into extruded lipid (EDOPC) solution: the endpoint correlates with the size of the titration increment

Titration in the opposite direction (DNA into lipid) showed less complicated behavior. As can be seen in Fig. 3, the slope, 694 ± 6 cal/mol DNA (averaged over all three runs made with the same lipid and DNA solutions), was independent of titration increment. On the other hand, the endpoint was sensitive to the titration increment and shifted toward higher charge ratios for the "larger increment" titrations. In agreement with previous observations (Kennedy et al., 2000) the endpoint was in the range of DNA/lipid charge ratio 0.2 to 0.6 (lipid/DNA = 1.5–5.0).

Formation of complex from vortexed EDOPC vesicles

Titration of lipid into DNA solution

The dependence of the binding enthalpy upon the titration increment is less obvious in the case of vortexed lipid. It can be related to the vesicle morphology, as discussed below, but it should also be emphasized that fewer experimental runs were done in this case. The binding enthalpy, averaged over six runs with different titration increments (from 1 to 15 steps to reach the neutrality), was 960 ± 170 cal/mol lipid, and the average endpoint was at a L:D charge ratio of 1.25 ± 0.22 (D:L = 0.82 ± 0.15).

Titration of DNA into lipid

As in the case of extruded lipid, the binding enthalpy was independent of titration increment and had the value of 680 ± 150 cal/mol DNA. Also as in the case of extruded lipid, the endpoint position was rate dependent, and had similar values, which varied from D:L = 0.26 to 0.69 (L:D = 3.8 to 1.4). The same correlation was also found, namely that the endpoint shifted to higher D:L charge ratios for "larger increment" titrations; this behavior is depicted in Fig. 4.

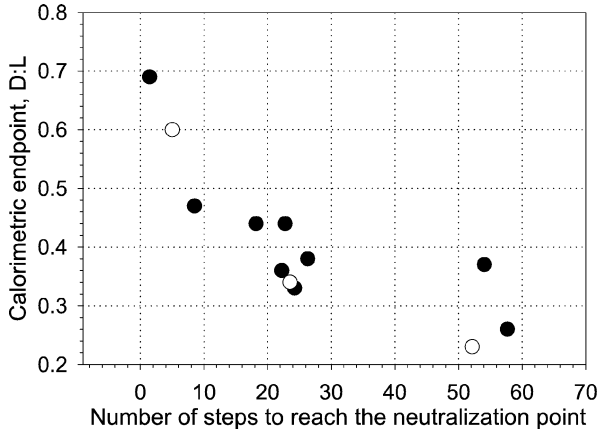

FIGURE 4 The calorimetric endpoint plotted against number of injections made to reach the neutralization point. DNA was titrated into EDOPC vesicle suspensions, either vortexed (●) or extruded (○). (T = 30°C, 150 mM HE-S).

DOTAP: the calorimetric profile is nonlinear when DNA is titrated into DOTAP

We used a DOTAP vesicle suspension that was sonicated. The effective vesicle size, determined by dynamic light scattering, was ~75 nm. Two runs were made with DOTAP titrated into DNA solution, for which the average binding enthalpy and endpoint were 446 ± 18 cal/mol lipid and L:D = 1.31 ± 0.14 (D:L = 0.76 ± 0.08), respectively. Three runs were made with the same lipid and DNA solutions for the opposite direction, and the average binding enthalpy and endpoint were 691 ± 69 cal/mol DNA and D:L = 0.43 ± 0.10 (L:D = 2.3 ± 0.5), respectively. Calorimetric curves for the case of DNA titration into lipid, presented in Fig. 5, illustrate two characteristic features of these experiments, 1) the endpoint strongly depends upon titration increment and 2) the calorimetric profile is nonlinear with the slope lower in the low charge ratio domain.

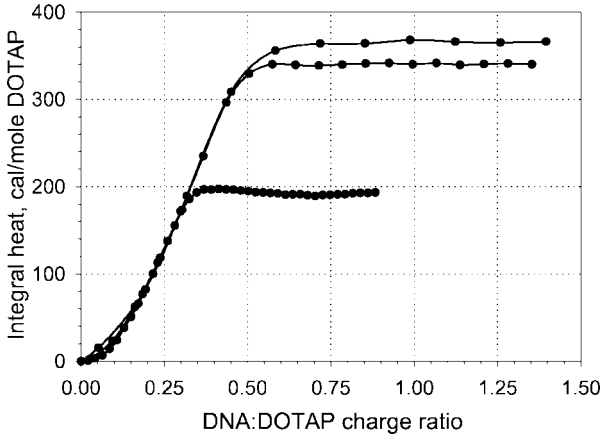

FIGURE 5 Titration of sonicated DOTAP vesicles with herring DNA.

DOTAP:DOPC mixture: lower enthalpy of binding to DNA

A sonicated (5 min, bath) equimolar mixture of DOTAP and DOPC was used in these experiments. The average size of vesicles was 78 ± 2 nm, as determined by dynamic light scattering. Two runs were made for each direction of titration. When lipid was injected into the DNA solution, the slope was 165 ± 28 cal/mol lipid, whereas for the opposite direction it was 351 ± 3 cal/mol DNA. The endpoints were L:D = 0.62 ± 0.10 and D:L = 0.36 ± 0.09, respectively (D:L = 1.6 ± 0.3 and L:D = 2.8 ± 0.7). The calorimetric profiles were nonlinear with increasing slope for the case when DNA was titrated into lipid solution, and the endpoint was rate dependent.

DOTAP:DOPE mixtures: interaction with DNA is exothermic

Low salt solution was used in this case to mimic as closely as possible previously published experimental conditions (Koltover et al., 1998). Two different mixtures of DOTAP and DOPE (DOPE weight fraction of 0.41 and 0.75) were prepared. All samples were sonicated 5 min. Results are summarized in Table 1 together with those of the other experiments described above.

Effect of ionic strength

The calorimetric profiles of complex formation between EDOPC and DNA obtained in buffer with different NaCl concentrations are presented in Fig. 6 (both lipid and DNA solutions had the same ionic strength). Both "small increment" and "large increment" titrations were done at each salt concentration. There was no qualitative difference between them, and only the "small increment" titrations are presented in the figure. Most of the curves fit the "two intersecting straight lines" model well with some minor nonlinearity at higher salt concentrations. On the other hand, there was a dramatic distortion of the shape of the calorimetric profile in the case of low salt. When lipid was titrated into DNA in low salt buffer, the integral enthalpy change reached a maximum at the endpoint, but then there was an exothermic step, and ~25% of originally absorbed heat were released. For the opposite direction of titration, there was a significant increase of slope before the endpoint, so that ~60% of the total heat was absorbed as a result of this late burst.

The average slope and the endpoint were calculated for all curves with appropriate corrections having been made in the case of nonlinearity. The results of fitting are presented in Fig. 7.

TABLE 1 Summary of calorimetry profiles obtained with different lipids

Lipid	Binding enthalpy, cal/mole		Endpoint	
	L→D, cal/mole lipid	D→L, cal/mole DNA	L→D, lipid/DNA	D→L, DNA/lipid
EDOPC, (extruded)*	720 ± 110	694 ± 6	1.33 ± 0.34	0.39 ± 0.19
EDOPC, (extruded)†	420 ± 90		1.22 ± 0.19	
EDOPC (vortexed)	960 ± 170	680 ± 150	1.25 ± 0.22	0.42 ± 0.12
DOTAP	446 ± 18	691 ± 69‡	1.31 ± 0.14	0.43 ± 0.10
DOTAP:DOPC, $\Phi_{DOPC} = 0.5$	165 ± 28	351 ± 3§	0.62 ± 0.10	0.36 ± 0.09
DOTAP:DOPE, $\Phi_{DOPE} = 0.41$	−1630 ± 80¶	−1530 ± 130‖**	1.10 ± 0.11	0.62 ± 0.14
DOTAP:DOPE, $\Phi_{DOPE} = 0.75$	−1790 ± 50	−1800 ± 110##	1.23 ± 0.09	0.42 ± 0.14

All runs were in 150 mM HE-S except DOTAP:DOPE mixtures, which were in HE. $T = 30°C$.
*"Large increment" titration.
†"Small increment" titration.
‡Nonlinear profile, binding enthalpy changed from 0.1 to 0.8 kcal/mol DNA.
§Nonlinear profile, binding enthalpy changed from 0.2 to 0.5 kcal/mol DNA.
¶Some heat was absorbed just prior to the endpoint.
‖Some extra heat is released after the endpoint, so that the calorimetric profile was completely flat only around the neutralization point.
**There was an increase of the absolute value of the slope prior to the endpoint.

DISCUSSION

We have studied the enthalpy of cationic lipid-DNA complex formation by isothermal titration calorimetry. The principle findings discussed below are: 1) mutual repulsion of DNA double strands within multilamellar lipoplex determines the energetics of complex formation; 2) in the presence of DOPE, complex formation was exothermic due to protonation of the PE amine group (the same idea was recently proposed by Lobo et al. (2001); 3) measurement of lipid-DNA affinities (high ionic strength); and 4) titration increment size and direction have important effects relative to DNA-coated vesicle morphology.

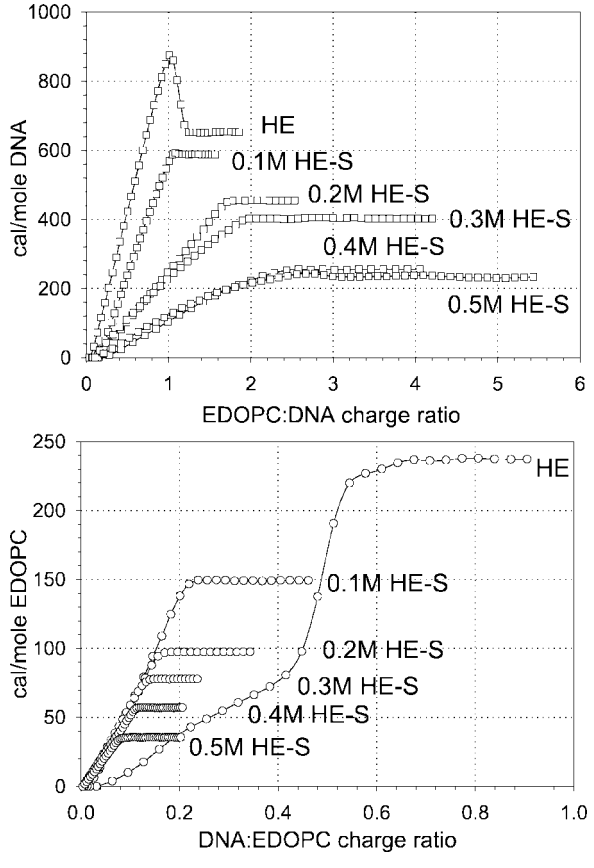

FIGURE 6 Calorimetric titrations made in 20 mM HEPES buffer with different NaCl content. (*Upper panel*) Titration of EDOPC into DNA solution; (*lower panel*) opposite direction.

Preliminary remarks: cationic lipid-DNA binding affinity and timescale

Cationic lipids exhibit strong binding to DNA even at moderate ionic strength, in contrast to DNA condensation by polyvalent cations (Matulis et al., 2000) and cationic surfactants (Spink and Chaires, 1997). The difference is due to the lamellar organization of the lipid with binding sites for an entire DNA double strand as a single unit. Macromolecular binding exhibits extremely high apparent affinity unless binding energy binding per monomeric unit is exceedingly small. Indeed, the apparent binding constant, K_{app}, is given by $K_{app} = N\exp(-N\Delta G_0/k_bT)$, in which N is the number of phosphate charges per DNA molecule ($2 \times$ number of base pairs), ΔG_0 is free energy change upon binding of individual charge. With $N \sim 2000$, the apparent binding affinity would be in the micromolar range only if $|\Delta G_0|$ were as small as $0.003\ k_bT$. Hence, all accessible DNA-lipid binding sites are saturated and any changes in binding enthalpy are directly attributable to changes of the complex energetics.

The timescale of ITC is a few minutes; significantly slower heat absorption/release is indistinguishable from instrumental drift. Therefore, absence of heat effects means

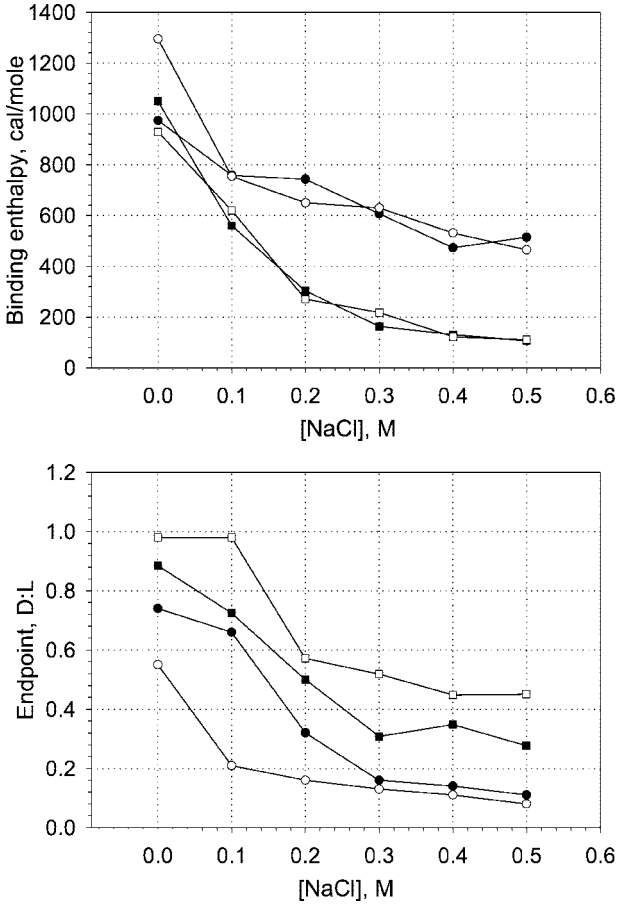

FIGURE 7 The binding enthalpy (*upper panel*) and the endpoint (*lower panel*) of the calorimetric profiles, obtained in buffers with different NaCl content. Designations: ■, lipid titrated into DNA solution, "large increment" titration; □, lipid titrated into DNA solution, "small increment" titration; ●, DNA titrated into lipid solution, "large increment" titration; ○, DNA titrated into lipid solution, "small increment" titration.

either there is no binding or that incorporation of added DNA/lipid requires a slow rearrangement of the complex. Accordingly, only relatively fast components of cationic lipid-DNA complex formation are visible by ITC.

Complex formation pathways as revealed by ITC

After initial contact (Barreleiro et al., 2000), cationic lipid-DNA complex formation can include a slow rearrangement, which affects transfection efficiency (Yang and Huang, 1998) and eventually leads to final multilamellar complex, well characterized both theoretically (Bruinsma, 1998; Dan, 1997; Harries et al., 1998; May et al., 2000) and structurally (Boukhnikachvilli et al., 1997; Gustafsson et al., 1995; Huebner et al., 1999; Koltover et al., 1999; Lasic et al., 1997; MacDonald et al., 1999a; Rädler et al., 1997; Templeton et al., 1997). Both physical (Kennedy et al., 2000; Xu et al., 1999) and biological properties (Zuidam et al., 1999; Rakhmanova, Pozharski, and MacDonald, in preparation) of lipoplexes are strongly influenced by the mode of preparation. Because kinetically trapped assemblies rather than equilibrium structures may determine biological efficiency, it is important to understand possible pathways of complex formation.

When DNA is titrated into lipid (~0.7 kcal/mol DNA (for both EDOPC and DOTAP; it is ~0.35 kcal/mol for the DOTAP:DOPC mixture)) the enthalpy change is that due to 1 mol of DNA charges entering the complex, inducing vesicle rupture, membrane mixing, and formation of a multilamellar complex (Huebner et al., 1999; Kennedy et al., 2000). For the opposite direction of titration, the binding enthalpy (per mole of added lipid) is ~1.6 times smaller (1.65 ± 0.35 with EDOPC and 1.55 ± 0.17 with DOTAP, however, it is 2.13 ± 0.36 with the DOTAP:DOPC mixture), as is expected from intermediate DNA-coated vesicles, in which one-half of the lipid is inaccessible to DNA. The lower binding enthalpy is also partly attributable to a decrease in DNA-DNA repulsion because DNA bound to monolayers has a larger spacing than in the lamellar complex, as shown by AFM (Fang and Yang, 1997; Clausen-Schaumann and Gaub, 1999).

The difference in binding enthalpies for opposite directions of titration vanishes when DNA is titrated with "large increments" of lipid that neutralize ~20% of the DNA charges upon the first injection (for "large/small increment" titrations, see Fig. 2). When lipid is injected in large portions, a local excess of lipid may exist long enough to induce vesicle rupture, leading to the formation of the equilibrium multilamellar complex.

Complex aggregation, not the true binding stoichiometry sets the calorimetric endpoint

Multilamellar lipoplexes always contain excess cationic charge unless a neutral helper lipid is included. Indeed, the projected area per base pair in the hydrated DNA double helix is ~85 $Å^2$ (3.5 Å (DNA length/base pair) × 24 Å (DNA diameter)), which is larger than area per lipid molecule for most of lipids (Marsh, 1990). It is not surprising therefore that, for both EDOPC and DOTAP, an excess of lipid was always observed at the calorimetric endpoint.

When DNA was titrated into lipid, the calorimetric endpoint (typically ~0.4, DNA:lipid charge (L:D ~ 2.5)) for all lipids under physiological salt conditions was significantly lower than that predicted from structural data (see Note 1) (Koltover et al., 1999). Moreover, the titration increment and calorimetric endpoint positions were strongly correlated (Fig. 4); "large increment" titrations gave higher endpoint D:L ratios than did "small increment" titrations. This indicates that the endpoint depends upon aggregation and is actually determined by the point where complex particles cannot readily accommodate additional material.

For lipid titrated into DNA, the calorimetric endpoint L:D charge ratio is ~1.3 (D:L ~ 0.8) and increases slightly with

increasing DNA concentration, which presumably means that coated vesicles are stabilized by higher DNA concentrations. The resulting delayed formation and aggregation of multilamellar lipoplexes is expected, because the probability of multilamellar complex formation is dictated by the rate of vesicle rupture (MacDonald et al., 1999b) relative to the rate of vesicle coating (Huebner et al., 1999; Kennedy et al., 2000). Because the rate of coating must depend largely upon diffusion, it increases with increased DNA concentration.

Nonlinear calorimetric profile of DNA titration into DOTAP: the possible measure of DNA-DNA mutual repulsion

EDOPC and DOTAP have similar enthalpies of binding to DNA (Table 1). However, when DNA was titrated into DOTAP suspensions, the calorimetric profile was nonlinear at low D:L values (Fig. 5) with the binding enthalpy increasing from 0.1 to 0.8 kcal/mol DNA, indicating that enthalpy depends upon charge ratio. We attribute the increase in enthalpy to the decrease in DNA spacing (Koltover et al., 1999) and corresponding increase in DNA-DNA mutual repulsion. The amplitude of the effect is close to the directly measured repulsive forces between parallel DNA double helices (Rau et al., 1984). DNA-DNA repulsion may thus dominate the binding enthalpy.

When DOTAP was titrated into DNA solution, the binding enthalpy did not depend upon charge ratio, an expected finding because DNA spacing does not increase significantly until the D:L charge ratio reaches 1.5 (L:D $\sim$ 0.7) (Koltover et al., 1999), which is above the calorimetric endpoint. Nonlinearity in calorimetric profiles was not observed for DNA titrations into EDOPC, so DOTAP and EDOPC differ significantly in their stoichiometry-structure relationships.

Helper lipid effect

A DOTAP:DOPC equimolar mixture exhibits qualitatively the same titration calorimetry profile as does pure DOTAP except that the enthalpy is lower. Because the DNA spacing (Koltover et al., 1999) is larger for the mixture, this again implicates DNA-DNA mutual repulsion as a major contribution to the enthalpy. In addition, when lipid is titrated into DNA, the calorimetric endpoint corresponds to an excess of DNA. The area of lipid membrane per cationic charge for this mixture is approximately twice that of pure DOTAP, so the complex can form with an excess of DNA. Accordingly, the endpoint corresponds to approximately one-half as much cationic lipid.

DOTAP:DOPE mixtures were examined to compare the thermodynamics of self-assembly of multilamellar and hexagonal complexes (Dan, 1998; Koltover et al., 1998; May and Ben-Shaul, 1997; May et al., 2000). We detected no calorimetric difference between lamellar phase lipid ($\Phi_{DOPE} = 0.41$) and hexagonal phase lipid ($\Phi_{DOPE} = 0.75$) (Koltover et al., 1998). In contrast to all other lipids we examined, complex formation with these lipids was exothermic.

Due to the positive surface charge, the effective pH on the surface of cationic liposomes is $\sim$11 at neutral bulk pH and low ionic strength (Banerjee et al., 1998; Zuidam and Barenholz, 1997). (The authors of the cited paper (Zuidam and Barenholz, 1997) used the same buffer system that we did: 20 mM HEPES at pH 7.5.) The $pK_a = 9.5$ of ethanolamine is well below 11, so DOPE in such bilayers is largely deprotonated. Because complex formation leads to a lower surface pH (Meidan et al., 2000; Zuidam et al., 1999; Zuidam and Barenholz, 1998), it must also lead to DOPE protonation. The latter is an exothermic process of $\sim$12 kcal/mol protons (Fasman, 1975), however some of that heat would be compensated by buffer ionization. (Recently, Middaugh and co-workers (Lobo et al., 2001) estimated the intrinsic, buffer-independent binding enthalpy for the DOTAP:DOPE mixture as ~ -5 kcal/mol with 0.5 proton exchanged with buffer. This gives $\sim$10 kcal/mol exothermic heat of DOPE protonation.) Hence, we suggest that changes in the protonation state of DOPE account for the exothermic nature of complex formation with these lipids. The important consequence of such DOPE protonation is that the entropic gain upon counterion release (Wagner et al., 2000) postulated to be the driving force of lipoplex formation (Bruinsma, 1998; Harries et al., 1998) is not necessary for DOTAP:DOPE mixtures. In other words, DOPE amine group protonation could be sole driving force of complex formation.

Complex formation at different ionic strengths

The calorimetric profile contains unusual features under low salt conditions (Fig. 6). When EDOPC was titrated into DNA, an exothermic process appeared just above the neutralization point. This probably reflects an increase of DNA spacing upon incorporation of extra lipid into an already-neutral complex. For the opposite direction of titration, the binding enthalpy was $\sim$0.2 cal/mol DNA for low D:L charge ratios and underwent an approximate fivefold, step-like increase at around D:L $\sim$ 0.45 (L:D $\sim$ 2.2). Significantly, this charge ratio corresponds to DNA spacing equal to twice the double strand diameter, so that the DNA subsequently added can insert between double strands in the preexisting grid, giving a much closer spacing and, therefore, a much larger binding enthalpy (see Note 2).

In 0.1 to 0.5 M NaCl, calorimetric profiles took the shape of two intersecting straight lines. The calorimetric endpoint for the titrations of DNA into EDOPC shifted toward lower

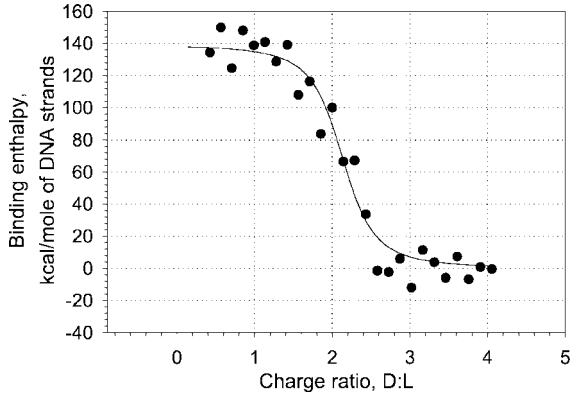

FIGURE 8 Extruded EDOPC vesicles titrated into herring DNA in 400 mM HE-S. Fitting is made by MicroCal Origin software, v.5.0., one binding site model.

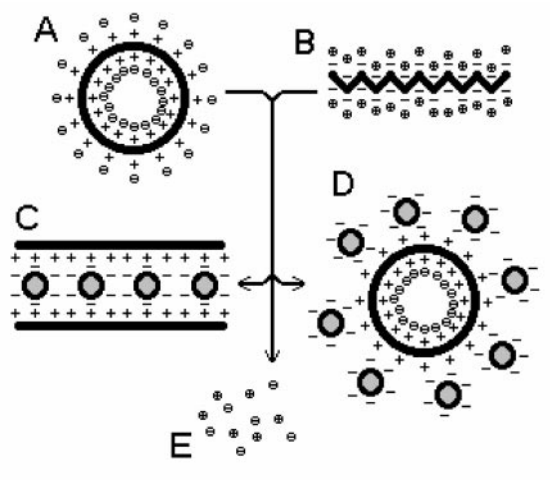

FIGURE 9 Diagram of cationic lipid-DNA complex formation. Circled pluses and minuses represent the counterions. (*A*) Unilamellar cationic lipid vesicle. (*B*) Naked DNA. (*C*) Multilamellar complex. (*D*) DNA-coated cationic lipid vesicle. (*E*) Released counterions.

D:L charge ratios with increasing salt concentration. This is expected because charge screening promotes aggregation, which, in turn, dictates that the endpoint depends on the titration increment (Fig. 7). The binding enthalpy decreases to ~0.5 kcal/mol DNA at the maximal ionic strength we explored, which is only 30% lower than the binding enthalpy at physiological salt conditions. Such a relatively small decrease is not surprising because in high ionic strength conditions, DNA-DNA repulsion is dominated by hydration forces, independent of salt concentration (Strey et al., 1998).

When EDOPC was titrated into DNA, the calorimetric endpoint shifted from D:L = 1.0 to 0.5 (L:D = 1.0 to 2.0) with increasing salt concentration, i.e., toward higher D:L charge ratios. Together with the divergence of binding enthalpies obtained for different directions of titration upon salt addition (Fig. 7), this indicates that increased salt concentration favors coated vesicle formation. This could result from a weakening of cationic lipid-DNA electrostatic interaction, which, in turn, would generate a weaker and less concentrated stress on the bilayer.

Cationic lipid-DNA complexes dissociate at high ionic strength (Kennedy et al., 2000; Mitrakos and Macdonald, 2000). The curvature of Fig. 6 similarly reveals dissociation at lower concentrations of vesicles. Fig. 8 shows the fit to a single site model, assuming that individual ~1-kb-long DNA molecules bind as a unit to the vesicle surface. The stoichiometry is D:L = 2.08 ± 0.05 (L:D = 0.48 ± 0.01), indicating that only one-half of the lipid binds DNA, presumably because of the inaccessibility of the inner monolayer of intact vesicles. Although the binding of an individual DNA charge is rather weak, with $K = 1.02 \pm 0.01\ M^{-1}$ ($\Delta H = 140 \pm 5$ cal/mol, $\Delta S = 0.50 \pm 0.02$ cal/mol *K*, per DNA charge), the apparent binding constant is in the micromolar range with whole DNA molecules binding fairly tightly (~15 kT per 1 kb).

DNA-DNA mutual repulsion: the major contributor to the cationic lipid-DNA binding enthalpy?

Arguments for dominance of DNA-DNA mutual repulsion in cationic lipid-DNA binding enthalpy are three: theoretical, based on ITC data, and comparison of ITC data to literature data on DNA double strand repulsion.

Assuming no structural changes of either lipid or DNA upon lipoplex formation, the enthalpy of the process (diagrammed in Fig. 9) reflects changes in the energy of the interactions among the three components, lipid, DNA, and counterions and is expressed as:

$$\Delta H = ((H_{LD} + H_{C(+)C(-)}) - (H_{LC(-)} + H_{DC(+)})) + (H_{DD} + H_{LL}) = \Delta H_a + \Delta Hr,$$

in which subscripts denote pairwise interactions (L for lipid, D for DNA, and C(+) and C(−) for counterions). H_{LD}, $H_{C(+)C(-)}$, $H_{LC(-)}$, and $H_{DC(+)}$ correspond to attractive forces and their combination, ΔH_a, reflects the change of the contribution of these forces to the overall enthalpy. If DNA-counterion and lipid-counterion attraction is effectively (in terms of enthalpy) replaced by DNA-lipid and counterion-counterion attraction, then ΔH_a may be close to zero. ΔH_r, in contrast, is purely repulsive and results from new interactions, namely, DNA-DNA (adjacent double strands) and lipid-lipid (adjacent bilayers) repulsion. An overall endothermic heat effect implies an increase in potential energy, such as from increased repulsion.

Several experimental observations can be rationalized in terms of DNA-DNA repulsion (based on the idea that any increase/decrease in binding enthalpy simply reflects decrease/increase of DNA spacing). These observations are: 1) differ-

ence in binding enthalpy for opposite directions of titration (attributed to different spacing of DNA inside lamellar complex versus on the vesicle surface); 2) similar values of binding enthalpy for DOTAP and EDOPC (these lipids have similar charge densities, so binding enthalpies should be similar, assuming DNA-DNA repulsion dominates); 3) nonlinearity of the calorimetric profile for DNA titration into DOTAP (enthalpy increases because progressive incorporation of DNA decreases strand separation); 4) decrease of binding enthalpy upon dilution of DOTAP by DOPC (DNA-DNA spacing increases with decreased bilayer charge density); 5) peculiarities of low ionic strength calorimetric profiles (titration of lipid into DNA gave an exothermal event beyond the neutralization point where DNA spacing should increase; titration of DNA into lipid gave a step-like increase of binding enthalpy at a stoichiometry where DNA double strands cannot be far apart); and 6) the ionic strength dependence of binding enthalpy (a relatively weak dependence is expected for DNA-DNA repulsion, which is governed by hydration forces, not electrostatics). Alternative explanations could be found for each of these effects, however, the proposed model provides a single explanation for all of them.

The contribution of DNA-DNA repulsion to the overall enthalpy of lipoplex formation, using the equation of state for DNA liquid crystals (Strey et al., 1997), is ~0.6 kcal/mol DNA (0.1 M NaCl, 25 Å; we did not take into account "fluctuation enhanced repulsion" because of its entropic nature). DNA-DNA repulsion can be somewhat different for the grid formed between two positively charged bilayers but not greatly, because the source of repulsion is water ordering within narrow area of close contact of double strands. Because the enthalpy of cationic lipid-DNA complex formation (~0.7 kcal/mol DNA), a process that brings DNA strands together, is similar to that of DNA-DNA repulsion, it appears likely that the latter dominates the overall binding enthalpy, whereas other contributions (involving substitution of like-sized interactions) compensate each other.

Bilayer-bilayer repulsion is negligible under our experimental conditions. Interbilayer separation in cationic lipid-DNA complexes is >20 Å (Rädler et al., 1997; Koltover et al., 1999; MacDonald et al., 1999a; Lin et al., 2000) and the interaction between two charged bilayers is repulsive and dominated by electrostatics at >10 to 20 Å (Marra, 1986; McDaniel and McIntosh, 1989; Loosley-Millman et al., 1982; Cowley et al., 1978; McIntosh et al., 1990). The electrostatic repulsion is much weaker than hydration forces that govern DNA-DNA interaction.

In summary, the hypothesis of the dominance of DNA-DNA repulsion in cationic lipid-DNA complex formation enthalpy is both useful in rationalizing experimental observations and consistent with theoretical expectations. This model may be attractive in theoretical studies of cationic lipid-DNA self-assembly because it allows approximating thermodynamic functions on the basis of well-studied DNA-DNA interactions.

NOTES

1. It is known from structural studies that DNA spacing is constant after some excess of DNA is reached (the same applies to the excess of lipid), which is attributed to the tightest possible packing of DNA strands in the lamellar complex. Accordingly, no more DNA could subsequently bind to the complex, which sets the upper limit for the calorimetric endpoint as well. However, this limit is at least the neutralization point, i.e., D:L = 1.

2. Projected area per pair of DNA charges ($Å^2$) in lamellar complex is $3.5d$, in which d is DNA spacing (Å). The corresponding area per pair of lipid charges (DNA strand is opposed by two monolayers within lamellar complex) is 77 $Å^2$. Hence, the relationship between DNA spacing and D:L charge ratio in the complex is given by $d = 77\ Å^2/(3.5\ Å\ (D:L)) = 22\ Å/(D:L)$. For (D:L)~0.45, we obtain $d \sim 49$ Å, which is ~2× hydrated DNA strand diameter (~24 Å).

This work was supported by the National Institutes of Health grant GM52329. We acknowledge the use of isothermal titration calorimetry and dynamic light scattering instruments in the Keck Biophysics Facility at Northwestern University. We thank Sidney Simon, Thomas McIntosh, and Ruby MacDonald for their suggestions that helped to improve the manuscript. We are also grateful to Adrian Parsegian and Helmut Strey for discussing with them issues related to the possible role of DNA-DNA interactions in cationic lipid-DNA complex formation.

REFERENCES

Banerjee, R., P. K. Das, and A. Chaudhuri. 1998. Interfacial indazolization: novel chemical evidence for remarkably high exo-surface pH of cationic liposomes used in gene transfection. *Biochim. Biophys. Acta.* 1373: 299–308.

Barreleiro, P. C. A., G. Olofsson, and P. Alexandridis. 2000. Interaction of DNA with cationic vesicles: a calorimetric study. *J. Phys. Chem. B.* 104:7795–7802.

Bartlett, J. R. 1959. Phosphorous assay in column chromatography. *J. Biol. Chem.* 234:466–468.

Boukhnikachvilli, T., O. Aguerre-Chariol, M. Airiau, S. Lesieur, M. Ollivon, and J. Vacus. 1997. Structure of in-serum transfecting DNA-cationic lipid complexes. *FEBS Lett.* 409:188–194.

Bruinsma, R. 1998. Electrostatics of DNA-cationic lipid complexes: isoelectric instability. *Eur. Phys. J. B.* 4:75–88.

Clausen-Schaumann, H., and H. E. Gaub. 1999. DNA adsorption to laterally structured charged lipid membranes. *Langmuir.* 15:8246–8251.

Cowley, A. C., N. L. Fuller, R. P. Rand, and V. A. Parsegian. 1978. Measurement of repulsive forces between charged phospholipid bilayers. *Biochemistry.* 17:3163–3168.

Dan, N. 1997. Multilamellar structures of DNA complexes with cationic liposomes. *Biophys. J.* 73:1842–1846.

Dan, N. 1998. The structure of DNA complexes with cationic liposomes: cylindrical or flat bilayers? *Biochim. Biophys. Acta.* 1369:34–38.

Fang, Y., and J. Yang. 1997. Two-dimensional condensation of DNA molecules on cationic lipid membranes. *J. Phys Chem.* 101:441–449.

Fasman, G. D., editor. 1975. Handbook of Biochemistry and Molecular Biology. Physical and Chemical Data, 3rd ed., Vol. 1. CRC Press, Cleveland. 162–164.

Felgner, P. L., T. R. Gadek, M. Holm, R. Roman, H. W. Chan, M. Wenz, J. P. Northrop, G. M. Ringold, and M. Danielsen. 1987. Lipofection: a highly efficient, lipid-mediated DNA transfection procedure. *Proc. Natl. Acad. Sci. U. S. A.* 84:7413–7417.

Gustafsson, J., G. Arvidson, G. Karlsson, and M. Almgren. 1995. Complexes between cationic liposomes and DNA visualized by cryo-TEM. *Biochim. Biophys. Acta.* 1235:305–312.

Harries, D., S. May, W. M. Gelbart, and A. Ben-Shaul. 1998. Structure, stability and thermodynamics of lamellar DNA-lipid complexes. *Biophys. J.* 75:159–173.

Hirsch-Lerner, D., and Y. Barenholz. 1999. Hydration of lipoplexes commonly used in gene delivery: follow-up by laurdan fluorescence changes and quantification by differential scanning calorimetry. *Biochim. Biophys. Acta.* 1461:47–57.

Huebner, S., B. J. Battersby, R. Grimm, and G. Cevc. 1999. Lipid-DNA complex formation: reorganization and rupture of lipid vesicles in the presence of DNA as observed by cryoelectron microscopy. *Biophys. J.* 76:3158–3166.

Kennedy, M. T., E. V. Pozharski, V. A. Rakhmanova, and R. C. MacDonald. 2000. Factors governing the assembly of cationic phospholipid-DNA complexes. *Biophys. J.* 78:1620–1633. [Correction: *Biophys. J.* 79:1168–1168.]

Koltover, I., T. Salditt, J. O. Rädler, and C. R. Safinya. 1998. An inverted hexagonal phase of cationic liposome-DNA complexes related to DNA release and delivery. *Science.* 281:78–81.

Koltover, I., T. Salditt, and C. R. Safinya. 1999. Phase diagram, stability, and overcharging of lamellar cationic lipid-DNA self-assembled complexes. *Biophys. J.* 77:915–924.

Koppel, D. E. 1972. Analysis of macromolecular polydispersity in intensity correlation spectroscopy: the method of cumulants. *J. Chem. Phys.* 57:4814–4820.

Kreiss, P., B. Cameron, R. Rangara, P. Mailhe, O. Aguerre-Charriol, M. Airiau, D. Scherman, J. Crouzet, and B. Pitard. 1999. Plasmid DNA size does not affect the physicochemical properties of lipoplexes but modulates gene transfer efficiency. *Nucleic Acid. Res.* 27:3792–3798.

Lasic, D. D., H. Strey, M. C. A. Stuart, R. Podgornik, and P. M. Frederik. 1997. The structure of DNA-liposome complexes. *J. Am. Chem. Soc.* 119:832–833.

Leventis, R., and J. R. Silvius. 1990. Interactions of mammalian cells with lipid dispersions containing novel metabolizable cationic amphiphiles. *Biochim. Biophys. Acta.* 1023:124–132.

Lin, A. J., N. L. Slack, A. Ahmad, I. Koltover, C. X. George, C. E. Samuel, and C. R. Safinya. 2000. Structure and structure-function studies of lipid/plasmid DNA complexes. *J. Drug Target.* 8:13–27.

Lobo, B. A., A. Davis, G. Koe, J. G. Smith, and C. R. Middaugh. 2001. Isothermal titration calorimetric analysis of the interaction between cationic lipids and plasmid DNA. *Arch. Biochem. Biophys.* 386:95–105.

Loosley-Millman, M. E., R. P. Rand, and V. A. Parsegian. 1982. Effects of monovalent ion binding and screening on measured electrostatic forces between charged phospholipid bilayers. *Biophys. J.* 40:221–232.

MacDonald, R. C., G. W. Ashley, M. M. Shida, V. A. Rakhmanova, Yu. S. Tarakhovsky, D. P. Pantazatos, M. T. Kennedy, E. V. Pozharski, K. A. Baker, R. D. Jones, H. S. Rosenzweig, K. L. Choi, R. Qiu, and T. J. McIntosh. 1999a. Physical and biological properties of cationic triesters of phosphatidylcholine. *Biophys. J.* 77:2612–2629.

MacDonald, R. C., M. T. Kennedy, A. Gorbonos, S. P. Pantazatos, M. M. Momsen, V. A. Rakhmanova, J. Stearns, and H. L. Brockman. 1999b. Properties of cationic phospholipids. *Biophys. J.* 76:A433.

MacDonald, R. C., R. I. MacDonald, B. P. M. Menco, K. Takeshita, N. K. Subbarao, and L. R. Hu. 1991. Small-volume extrusion apparatus for preparation of large, unilamellar vesicles. *Biochim. Biophys. Acta.* 1061: 297–303.

Marra, J. 1986. Direct measurement of the interaction between phosphatidylglycerol bilayers in aqueous electrolyte solutions. *Biophys. J.* 50: 815–825.

Marsh, D. 1990. CRC Handbook of Lipid Bilayers. CRC Press, Boca Raton, FL. 163–184.

Matulis, D., I. Rouzina, and V. A. Bloomfield. 2000. Thermodynamics of DNA binding and condensation: isothermal titration calorimetry and electrostatic mechanism. *J. Mol. Biol.* 296:1053–1063.

May, S., and A. Ben-Shaul. 1997. DNA-lipid complexes: stability of honeycomb-like and spaghetti-like structures. *Biophys. J.* 73:2427–2440.

May, S., D. Harries, and A. Ben-Shaul. 2000. The phase behavior of cationic lipid-DNA complexes. *Biophys. J.* 78:1681–1697.

McDaniel, R. V., and T. J. McIntosh. 1989. Neutron and X-ray diffraction structural analysis of phosphatidylinositol bilayers. *Biochim. Biophys. Acta.* 983:241–246.

McIntosh, T. J., A. D. Magid, and S. A. Simon. 1990. Interactions between charged, uncharged, and zwitterionic bilayers containing phosphatidylglycerol. *Biophys. J.* 57:1187–1197.

Meidan, V. M., J. S. Cohen, N. Amariglio, D. Hirsch-Lerner, and Y. Barenholz. 2000. Interaction of oligonucleotides with cationic lipids: the relationship between electrostatics, hydration and state of aggregation. *Biochim. Biophys. Acta.* 1464:251–261.

Mitrakos, P., and P. M. Macdonald. 2000. Nucleotide chain length and the morphology of complexes with cationic amphiphiles: ^{31}P-NMR observations. *Biochim. Biophys. Acta.* 1463:355–373.

Oberle, V., U. Bakowsky, I. S. Zuhorn, and D. Hoekstra. 2000. Lipoplex formation under equilibrium conditions reveals a three-step mechanism. *Biophys. J.* 79:1447–1454.

Pector, V., J. Backmann, D. Maes, M. Vandenbranden, and J.-M. Ruysschaert. 2000. Biophysical and structural properties of DNA/DIC_{14}-amidine complexes: influence of the DNA/lipid ratio. *J. Biol. Chem.* 275:29533–29538.

Rädler, J. O., I. Koltover, T. Salditt, and C. R. Safinya. 1997. Structure of DNA-cationic liposome complexes: DNA intercalation in multilamellar membranes in distinct interhelical packing regimes. *Science.* 275: 810–814.

Rau, D. C., B. Lee, and V. A. Parsegian. 1984. Measurement of the repulsive force between polyelectrolyte molecules in ionic solution: hydration forces between parallel DNA double helices. *Proc. Natl. Acad. Sci. U. S. A.* 81:2621–2625.

Ross, P. C., and S. W. Hui. 1999. Lipoplex size is a major determinant of in vitro lipofection efficiency. *Gene Ther.* 6:651–659.

Spink, C. H., and J. B. Chaires. 1997. Thermodynamics of the binding of a cationic lipid to DNA. *J. Am. Chem. Soc.* 119:10920–10928.

Strey, H. H., V. A. Parsegian, and R. Podgornik. 1997. Equation of state for DNA liquid crystals: fluctuation enhanced electrostatic double layer repulsion. *Phys. Rev. Lett.* 78:895–898.

Strey, H. H., R. Podgornik, D. C. Rau, and V. A. Parsegian. 1998. DNA-DNA interactions. *Curr. Opin. Struct. Biol.* 8:309–313.

Templeton, N. S., D. D. Lasic, P. M. Frederik, H. H. Strey, D. D. Roberts, and G. N. Pavlakis. 1997. Improved DNA:liposome complexes for increased systemic delivery and gene expression. *Nat. Biotechnol.* 15: 647–652.

Wagner, K., D. Harries, S. May, V. Kahl, J. O. Rädler, and A. Ben-Shaul. 2000. Direct evidence for counterion release upon cationic lipid-DNA condensation. *Langmuir.* 16:303–306.

Wiseman, T., S. Williston, J. F. Brandts, and L.-N. Lin. 1989. Rapid measurement of binding constants and heats of binding using a new titration calorimeter. *Anal. Biochem.* 179:131–137.

Xu., Y., S.-W. Hui, P. Frederik, and F. C. Szoka, Jr. 1999. Physicochemical characterization and purification of cationic lipoplexes. *Biophys. J.* 77: 341–353.

Yang, J.-P., and L. Huang. 1997. Overcoming the inhibitory effect of serum on lipofection by increasing the charge ratio of cationic liposome to DNA. *Gene Ther.* 4:950–960.

Yang, J.-P., and L. Huang. 1998. Time-dependent maturation of cationic liposome-DNA complex for serum resistance. *Gene Ther.* 5:380–387.

Zantl, R., L. Baicu, F. Artzner, I. Sprenger, G. Rapp, and J. O. Rädler. 1999. Thermotropic phase behavior of cationic lipid-DNA complexes compared to binary lipid mixtures. *J. Phys. Chem. B.* 103:10300–10310.

Zuidam, N. J., and Y. Barenholz. 1997. Electrostatic parameters of cationic liposomes commonly used for gene delivery as determined by 4-heptadecyl-7-hydroxycoumarin. *Biochim. Biophys. Acta.* 1329:211–222.

Zuidam, N. J., and Y. Barenholz. 1998. Electrostatic and structural properties of complexes involving plasmid DNA and cationic lipids commonly used for gene delivery. *Biochim. Biophys. Acta.* 1368:115–128.

Zuidam, N. J., D. Hirsch-Lerner, S. Margulies, and Y. Barenholz. 1999. Lamellarity of cationic liposomes and mode of preparation of lipoplexes affect transfection efficiency. *Biochim. Biophys. Acta.* 1419:207–220.